



HAL
open science

BAG6 promotes PINK1 signaling pathway and is essential for mitophagy

Romain Ragimbeau, Leila El Kebriti, Salwa Sebti, Elise Fourgous, Abdelhay Boulahtouf, Giuseppe Arena, Lucile Espert, Andrei Turtoi, Céline Gongora, Nadine Houédé, et al.

► **To cite this version:**

Romain Ragimbeau, Leila El Kebriti, Salwa Sebti, Elise Fourgous, Abdelhay Boulahtouf, et al.. BAG6 promotes PINK1 signaling pathway and is essential for mitophagy. *FASEB Journal*, 2021, 35 (2), 10.1096/fj.202000930R . hal-03405271

HAL Id: hal-03405271

<https://hal.science/hal-03405271v1>

Submitted on 27 Oct 2021

HAL is a multi-disciplinary open access archive for the deposit and dissemination of scientific research documents, whether they are published or not. The documents may come from teaching and research institutions in France or abroad, or from public or private research centers.

L'archive ouverte pluridisciplinaire **HAL**, est destinée au dépôt et à la diffusion de documents scientifiques de niveau recherche, publiés ou non, émanant des établissements d'enseignement et de recherche français ou étrangers, des laboratoires publics ou privés.

BAG6 promotes PINK1/PARKIN signaling and is essential for mitophagy induction in a LIR dependent manner

Romain Ragimbeau¹, Leila El Kebriti^{1,2}, Salwa Sebti^{3,4}, Elise Fourgous¹, Abdelhay Boulahtouf¹, Giuseppe Arena³, Lucile Espert⁵, Andrei Turtoi¹, Céline Gongora¹, Nadine Houédé^{1,2}, Sophie Pattingre^{1, ‡}

1: IRCM, Institut de Recherche en Cancérologie de Montpellier, INSERM U1194, Université de Montpellier, Institut régional du Cancer de Montpellier, Montpellier, F-34298, France.

2: CHU de Nîmes, F-30900 Nîmes;

3: Center for Autophagy Research, University of Texas Southwestern Medical Center, Dallas, TX, USA.

4: Department of Internal Medicine, University of Texas Southwestern Medical Center, Dallas, TX, USA.

3: Luxembourg Center for Systems Biomedicine, University of Luxembourg, 6, avenue du Swing, L-4367 Belvaux, Luxembourg;

5: IRIM, University of Montpellier, UMR 9004 CNRS, 34293 Montpellier, France.

‡ Corresponding author: sophie.pattingre@inserm.fr

Keywords: Mitophagy, BAG6, Signaling, Receptor

Abbreviations

ATG proteins	Autophagy-related proteins
BAG6	Bcl-2-associated Athanogen-6
BNIP3	BCL2-interacting protein 3
CCCP	Carbonyl Cyanide m-ChloroPhenyl hydrazine
DMEM	Dulbecco's Modified Eagle's Medium
DRP1	Dynamin-Related Protein 1
EBSS	Earle's Balanced Salt Solution
EV	Empty Vector
ER	Endoplasmic Reticulum
FCS	Fetal Calf Serum
IMM	Inner Mitochondrial Membrane
LC3	protein light chain 3
LIR	LC3 Interacting Region
LoVo cells transfected with BAG6	LoVo-BAG6
MEFs	Mouse Embryonic Fibroblast
MFN2	MitoFusiN-2
NIX	NIP3-like protein X
NT	Non Treated
OMM	Outer Mitochondrial Membrane
PINK1	PTEN-Induced putative Kinase 1
PK	Proteinase K
TFAM	Transcription Factor A, Mitochondrial
TOMM20	Translocase of Outer Mitochondrial Membrane 20

BAG6 promotes PINK1/PARKIN signaling and is essential for mitophagy induction in a LIR dependent manner

Abstract

Bcl-2-associated athanogen-6 (BAG6) is a nucleocytoplasmic shuttling protein involved in protein quality control. We previously demonstrated that BAG6 is essential for autophagy by regulating the intracellular localization of the acetyltransferase EP300 and thus modifying accessibility to its substrates: (TP53 in the nucleus and autophagy-related proteins in the cytoplasm). Here, we investigated BAG6 localization and function in the cytoplasm. First, we demonstrated that BAG6 is localized in the mitochondria. Specifically, BAG6 is expressed in the mitochondrial matrix under basal conditions, and translocates to the outer mitochondrial membrane after mitochondrial depolarization with carbonyl cyanide m-chlorophenyl hydrazine, a mitochondrial uncoupler that induces mitophagy. In SW480 cells, the down regulation of BAG6 abrogates its ability to induce mitophagy and PINK1 accumulation. On the reverse, its ectopic expression in LoVo colon cancer cells, which do not express endogenous BAG6, reduces the size of the mitochondria, induces mitophagy, leads to the activation of the PINK1/PARKIN pathway and to the phospho-ubiquitination of mitochondrial proteins. Finally, BAG6 contains two LIR (LC3-interacting Region) domains specifically found in receptors for selective autophagy and responsible for the interaction with LC3 and for autophagosome selectivity. Site-directed mutagenesis showed that BAG6 requires wild type LIRs domains for its ability to stimulate mitophagy. In conclusion, we propose that BAG6 is a novel mitophagy receptor that induces PINK1/PARKIN signaling and mitophagy in a LIR dependent manner.

Introduction

Mitochondria are found in the cytoplasm of all eukaryotic cells, and are essential for the maintenance of cell homeostasis. They provide energy through ATP production *via* oxidative phosphorylation, and are involved in many crucial cell functions, such as signaling, metabolism, calcium homeostasis and intrinsic apoptosis. Due to their major functions in cell fate and homeostasis, the structure, biogenesis and degradation of mitochondria need to be tightly regulated. Mitochondria are highly dynamic organelles that oscillate constantly between fusion and fission, depending on the cellular needs. For instance, the lysosomal degradation of mitochondria only occurs when the organelles are fragmented, which facilitates their engulfment by autophagosomes [1–3].

Macroautophagy, called thereafter autophagy, is regulated by autophagy-related proteins (ATG) and allows the degradation of intracellular material into the lysosomes after its sequestration in a vacuole, called autophagosome. Autophagy occurs in physiological conditions and ensures cellular homeostasis by renewing the cytoplasm. It is also a stress response mechanism and its induction allows cell survival. Upon stress, a selective form of autophagy enables the specific degradation of aggregates (aggrephagy), organelles (e.g. pexophagy in the case of peroxisomes), or intracellular pathogens (xenophagy). Organelles are selectively targeted to autophagosomes through receptors or adaptors that bind to autophagosomal bound form of protein light chain 3 (LC3). These receptors/adaptors harbor a LC3 Interacting Region (LIR domain) defined by the W/F/YxxL/I sequence that is essential for the interaction with LC3-II [4].

On the other hand, mitophagy is the process by which damaged or depolarized mitochondria are degraded through selective autophagy. It has been shown that several

mitophagic receptors, located on mitochondria, participate in this process, including BNIP3L/NIX [5], BNIP3 [6], BCL2L13 [7], PHB2 [8], and FKBP8 [9] in mammalian cells, as well as Atg32 in yeast [10].

The specific degradation of mitochondria is also ensured by cytoplasmic adaptors [5] that can bring together the autophagosome, *via* LC3, and the mitochondria via specific signaling events [11]. Upstream of the core mitophagy machinery, the most characterized signaling pathway specific for mitophagy induction involves the PTEN-induced putative kinase 1 (PINK1) and the E3 ubiquitin protein ligase PARKIN. After mitochondrial depolarization, PINK1 accumulates at the outer mitochondrial membrane (OMM) and activates PARKIN by phosphorylation, thus allowing its mitochondrial recruitment [12]. Once activated, PARKIN ubiquitinates OMM proteins and then PINK1 phosphorylates ubiquitin on serine 65 [13]. Then, specific adaptors, such as Sequestosome 1/P62, can recognize the tagged mitochondria for autophagic elimination.

Bcl-2-associated athanogen-6 (BAG6; also known as BAT3/Scythe) is a nucleocytoplasmic shuttling ubiquitin-like protein involved in many physiological and pathological processes, such as apoptosis, antigen presentation and T-cell response. It acts as a co-chaperone for HSP/HSC70 proteins to allow the recognition of misfolded proteins and their proteasomal degradation [14,15]. We previously demonstrated that BAG6 is essential for autophagy by regulating the intracellular localization of the acetyltransferase EP300, thus modifying accessibility to its substrates (TP53 in the nucleus, and ATG5, AGT7, ATG12 and LC3 in the cytoplasm). During autophagy induction, BAG6 sequesters EP300 in the nucleus, leading to increased acetylation of TP53 and expression of pro-autophagic TP53 target genes. The reduced EP300 level in the cytoplasm maintains a low level of cytoplasmic ATG protein acetylation that allows autophagy induction [16,17]. It has been recently reported that BAG6

has a role also in the physiology of mitochondria. Specifically, BAG6 is involved in the proteasomal degradation of the OMM GTPases mitofusin 1 and 2 (MFN1 and 2) in cells that do not express Dynamin-Related Protein 1 (DRP-1), a protein involved in mitochondrial fission [18]. BAG6 is also involved in the PARKIN-dependent cytoplasmic redistribution of damaged mitochondria [19].

In this work, we investigated BAG6 role in the regulation of mitophagy after mitochondrial depolarization. We first demonstrated that BAG6 is present in the mitochondria of all the tested cell lines (SW480, MEFs, HEK293T and in BAG6-transfected null cells LoVo). Then, we observed that BAG6 plays a crucial role in all the steps of mitophagy execution. Indeed, BAG6 regulated the mitochondrial structure and induced fission, a prerequisite for mitophagy. BAG6 stimulated PINK1/PARKIN signaling and ubiquitin phosphorylation on mitochondrial proteins. Finally, we found that BAG6 harbors two LIR domains, LIR1 (N-terminal position) and LIR2 (C-terminal position). After site directed mutagenesis, we demonstrated that both LIR domains are essential for mitophagy induction. In addition, when mutated on its LIR2 domain, BAG6 loses its interaction with LC3 suggesting that it may behave like a mitophagy adaptor or receptor.

Results

BAG6 is localized in mitochondria

To investigate BAG6 role in mitophagy, we first analyzed its intracytoplasmic localization after subcellular fractionation in SW480 colon cancer cells. We observed that BAG6 was present in the mitochondrial fraction, similarly to the matrix mitochondrial marker the Mitochondrial Transcription Factor A (TFAM) (Fig. 1A) and the Outer membrane mitochondrial marker Translocase of Outer Mitochondrial Membrane 20 (TOMM20) (Fig. S1A). In SW480 cells, BAG is also located to the nucleus (Fig S1B). By subcellular fractionation, we noticed that endogenous BAG6 was also localized in mitochondria in HEK293T cells (Fig. S1C) and in mouse embryonic fibroblasts (MEFs) (Fig. S1D). Immunofluorescence staining of SW480 cells confirmed BAG6 co-localization with TOMM20 (Fig 1B).

To precisely determine BAG6 sub-mitochondrial localization, we carried out limited proteolysis of isolated mitochondria from SW480 cells to sequentially degrade mitochondrial membranes. Specifically, incubation with proteinase K (PK) leads to OMM degradation, while PK and swelling target the inner mitochondrial membrane (IMM), and PK, swelling and Triton X-100 degrade the entire mitochondria [20]. In basal conditions, the BAG6 protein displayed a degradation pattern similar to that observed for the Mitochondrial Transcription Factor A (TFAM), indicative of its localization in the mitochondrial matrix (Fig. 1C).

Human LoVo cells do not express BAG6 (Fig. 1D). Subcellular fractionation of BAG6-transfected LoVo cells confirmed the presence of BAG6 in the mitochondrial fraction (Fig. 1D). In LoVo cells transfected with BAG6 (LoVo-BAG6), BAG6 was also located to the nucleus (Fig S1E). As BAG6 may also be localized in the Endoplasmic Reticulum (ER) [21], we incubated the different cell fractions with calnexin, an ER marker, to exclude the presence of

mitochondrion-associated ER membranes in the mitochondrial fraction (Fig. 1D). Immunofluorescence staining of LoVo-BAG6 cells confirmed BAG6 co-localization with TOMM20 (Fig 1E).

After limited proteolysis of isolated mitochondria from BAG6-expressing LoVo cells cultured in complete media (NT), BAG6 resistance to PK treatment and swelling suggested again that BAG6 was localized in the mitochondrial matrix. Conversely, after induction of mitochondrial depolarization with carbonyl cyanide m-chlorophenyl hydrazine (CCCP), BAG6 was degraded upon incubation with PK alone, like the OMM protein TOMM20 (Fig. 1F).

BAG6 does not possess a transmembrane domain or a canonical mitochondrial targeting signal, and the mechanism of its targeting to mitochondria remains unknown. We cannot exclude that BAG6 interacts with a cytoplasmic co-factor responsible for its transport to the TOMM20 complex. Indeed, yeast two hybrid screening using TOMM20 as bait showed that BAG6 interacts with TOMM20 [35] and our preliminary investigations demonstrates that BAG6 interacts with TOMM20 by co-immunoprecipitation (Fig. S2).

To summarize, these results demonstrate that BAG6 is located into the mitochondria in all the cell lines tested and more precisely in the mitochondrial matrix in basal conditions, and in the OMM after mitochondrial damage.

BAG6 induces mitochondrial morphological changes and mitophagy

Mitochondria are dynamic organelles whose homeostasis is tightly regulated by a balance between biogenesis and degradation. Recently, it has been suggested that BAG6 might have a role in mitochondrial morphology through its interaction and ability to modulate the turnover of the GTPase MFN2, a mitochondrial protein involved in fusion [18]. Moreover, mitochondrial fission is considered as a pre-requisite for mitophagy [1]. On the basis of our findings that

BAG6 has a role in autophagy [16,17] and is relocated to the OMM after incubation with CCCP (Fig. 1F), we asked whether BAG6 participates in the maintenance of the mitochondrial morphology and mass and in mitophagy.

First, we performed a morphological analysis by transmission electron microscopy (TEM) of LoVo cells transfected with empty vector (EV) or a BAG6-encoding plasmid after incubation in the presence or absence of CCCP (Fig. 2A). First, to investigate BAG6 role in mitochondrial morphology, we measured the size of 200 mitochondria using ImageJ software and observed that their size was significantly decreased in BAG6-expressing cells, independently of CCCP treatment (Fig. 3B). Although significant, this result are underestimated because of the random selection of longitudinal cross-sectioned mitochondria and the partial transfection efficiency of LoVo cells (40% efficiency – see methods). During mitochondrial fission, the cytosolic GTPase DRP1 translocates to the mitochondria and is phosphorylated on serine 616. To further confirm the role of BAG6 in mitochondrial fission, cell fractionation of EV- or BAG6-transfected LoVo cells showed that DRP1 and its phosphorylated active form accumulated only in mitochondria of BAG6-transfected cells (Fig. S3A, S3B). Altogether, these data suggest that BAG6 induces mitochondrial fission. In order to monitor the role of BAG6 in mitochondrial mass, the quantification of the number of mitochondria in 200 cells indicated that their number per cell was significantly decreased in BAG6-expressing cells after exposure to CCCP suggesting that BAG6 is involved in mitochondrial mass regulation (Fig. 2C).

Next, we assessed the role of BAG6 in mitophagy regulation by using chloroquine (CQ), an inhibitor of autophagic flux that impairs the fusion between autophagosome and lysosome. TFAM, a mitochondrial matrix marker, is commonly used to monitor the degradation of mitochondria by mitophagy because OMM and IMM markers might also be degraded through the proteasome pathway [8,23,24]. After incubation with CCCP, TFAM expression was reduced by 58% in BAG6-expressing LoVo cells compared with control (EV) (Fig. 2E, 2F).

Co-incubation with CQ restored TFAM expression level in BAG6-expressing cells to what observed in control cells (untreated EV), showing that mitophagy is involved in BAG6-dependent degradation of TFAM (Fig. 2E, 2F).

To specifically conclude about the role of BAG6 in mitophagy, we downregulated BAG6 expression in SW480 cells by shRNA approach. Thus, the mitochondrial staining using anti TOMM-20 antibody of shluc-SW480 and shBAG6-SW480 cells after incubation with CCCP showed that the measurement of TOMM puncta, which reflects the mitochondrial mass, was decreased only in BAG6-expressing cells, confirming that BAG6 is involved in mitochondrial mass regulation (Fig. 3A, 3B). We next measured mitophagy by assaying the expression of TFAM by western blot. After incubation with CCCP, TFAM expression was two fold reduced in shLUC-SW480 cells compared with shBAG6-SW480 cells (Fig. 3C, 3D). Co-incubation with CQ restored TFAM expression level in BAG6-expressing cells to what observed in cells with reduced BAG6 expression (shBAG6), showing that mitophagy is involved in BAG6-dependent degradation of TFAM (Fig. 3C, 3D).

Altogether, these findings indicate that BAG6 is essential for mitophagy induction after mitochondrial depolarization.

The PINK1/PARKIN pathway is activated during BAG6-dependent mitophagy

Since cccp may have a non specific effect on pink1 we used an alternative mitophagy inducer in sw480 to assess the accumulation of pink1 After incubation with a mix of oligomycin (inhibitor of ATP synthase) and antimycin (inhibitor of the Complex III of the respiratory chain),

Mitophagy induction requires precise signaling events that target the mitochondria for their lysosomal degradation. Specifically, after membrane depolarization, the mitochondrial kinase PINK1 is stabilized at the OMM where it recruits the E3 ubiquitin-protein ligase PARKIN. Then, PINK1 and PARKIN cooperate to assemble phosphorylated ubiquitin chains (S65-phospho-ub) on proteins at the OMM that in turn recruit adaptors. Adaptors bind to S65-phospho-ub mitochondrial proteins through their ubiquitin-binding/ubiquitin-associated (UBD/UBA) domain, and to LC3-II via their LIR domain. Alternatively, mitophagy also relies on integral mitochondrial membrane receptors that contain a LIR domain, such as PHB2, FUNDC1, NIX, BNIP3, and BCL2L13 [5,7,8,25,26]. In this case, the PINK1/PARKIN pathway should be dispensable. However, some mitochondrial receptors, such as PHB2, use the PINK1/PARKIN pathway to enhance mitophagy induction or to induce the OMM proteasomal degradation [8].

Many recent studies reported the role of the BAG family member, including BAG6, in the accumulation of PINK1 through direct interaction ([ref 28 29 32 et ajouter chu](#)). In SW480 WT cells, we noticed an interaction between BAG6 and PINK1 (Fig 4A). After deleting BAG6 expression in SW480 cells we observed a decreased expression of PINK1 in shBAG6-SW480 cells suggesting that BAG6 may stabilize PINK1 expression (Fig 4B, 4C).

To further determine the role of the PINK1/PARKIN pathway in BAG6-dependent mitophagy, we showed that BAG6 expression in LoVo cells promoted PINK1/PARKIN mitochondrial localization in LoVo cells (Fig. 4D, 4E). Then, using an antibody against ubiquitinated proteins phosphorylated on S65 we observed a 40% increase in the level of S65-phospho-ub mitochondrial proteins in BAG6-transfected LoVo cells compared with EV-transfected cells

after incubation with CCCP (Fig. 4D, 4E). All together, these results suggest that BAG6 stabilizes PINK1 and stimulates the PINK1/PARKIN pathway after mitochondrial damages.

The LIR2 domain of BAG6 is responsible for its interaction with LC3 and for mitophagy induction

Our data showed that BAG induces mitophagy, mitochondrial fission, and the PINK1/PARKIN pathway. To further investigate the mechanism by which BAG6 stimulates mitophagy, we analyzed BAG6 sequence and observed the presence of two LIR domains (amino acids 274-279 named LIR1 and 1016-1021 named LIR2) (<https://ilir.warwick.ac.uk/index.php>,[4]) (Fig. 5A). LIR domains have a conserved consensus signal of six amino acids required for the interaction with LC3-II. Receptor or adaptor proteins bearing an inactivating mutation in their LIR domain cannot interact with LC3-II, leading to mitophagy inhibition.

By subcellular fractionation, we first verified that BAG6 variants with mutations in the first (BAG6 LIR1) or second LIR domain (BAG6 LIR2) showed a mitochondrial localization such as WT BAG6 (Fig 5B).

Next, we investigated the role of BAG6 LIR domains in mitochondrial mass regulation after incubation or not with CCCP by TEM. By counting the number of mitochondria per cell, we observed that their number was similarly reduced in WT BAG6- and BAG6 LIR1-transfected LoVo cells. Conversely, CCCP effect on mitochondrial mass was less important in BAG6 LIR2-transfected cells (Fig. 5C, 5D).

To determine whether BAG6 mutants affects mitochondrial mass through mitophagy, we analyzed TFAM expression in LoVo cells transfected with EV, WT BAG6, BAG6 LIR1 or BAG6 LIR2 (Fig. 5E, 5F). As previously showed, after incubation with CCCP, TFAM expression was decreased in WT BAG6 cells compared with control (EV). Conversely, TFAM

strongly accumulated both in BAG6 LIR1 and BAG6 LIR2-transfected cells after incubation with CCCP, suggesting that the LIR mutation inhibited TFAM degradation.

Finally, to test whether BAG6 interacts with LC3 through its LIR domains, we transfected LoVo cells with EV, wild type (WT) BAG6, or BAG6 variants with mutations in the first (BAG6 LIR1) or second LIR domain (BAG6 LIR2) (Fig. 5A). After immunoprecipitation with an anti-BAG6 antibody, analysis with an anti-LC3b antibody showed that WT BAG6 and BAG6 LIR1 interacted with LC3, but not BAG6 LIR2 (Fig. 5G). This data suggests that BAG6 might act as a mitophagy receptor or adaptor.

These data showed that the LIR domains are essential for BAG6 dependent mitophagy. LIR2 domain of BAG6 is crucial for its interaction with LC3 and for its pro-mitophagy effect and suggests that BAG6 is a new mitophagy receptor or adaptor.

Discussion

In this work, we described a new function for the co-chaperone BAG6. Specifically, BAG6 is localized in mitochondria and regulates mitophagy by acting at different steps of this process. Indeed, when ectopically expressed in LoVo cells, BAG6 induced mitochondrial fragmentation, considered a prerequisite for mitochondrial engulfment into autophagosomes [27]. In these cells, BAG6 expression also led to a reduction of the mitochondrial mass in a chloroquine-dependent manner, indicating that BAG6 induces mitophagy. BAG6 also induced PINK1/PARKIN signaling after mitochondrial depolarization and the phosphorylation-ubiquitination of mitochondrial proteins, an “eat me signal” for mitophagy. Finally, the BAG6 sequence includes two LIR domains that are considered essential for the interaction with LC3 and the selective sequestration of mitochondria in autophagosomes [4]. Using site-directed mutagenesis, we found that LIR1 and LIR2 domains are essential for mitochondrial degradation even if the interaction between BAG6 LIR1 and LC3 is maintained. However, the LIR2 domain of BAG6 is required for both its interaction with LC3 and mitophagy induction suggesting that BAG6 is a new mitophagy receptor or adaptor. The mechanism by which the LIR1 domain of BAG6 modulates mitophagy requires additional studies.

Recent literature data also showed that BAG6 is important for the maintenance of mitochondrial physiology. Indeed, in the absence of DRP1 (i.e. in conditions that favor mitochondrial fusion), BAG6 allows the degradation of MNF2, probably to suppress fusion events [18]. It would be interesting to determine the role of BAG6-mediated proteasomal degradation of MNF2 in mitophagy, especially because OMM proteasomal degradation is an early event in mitophagy [8,24].

It is also established that BAG6 is important for the cytoplasmic redistribution of damaged mitochondria in a PARKIN-dependent manner [19]. Interestingly, other BAG family

members are also involved in PINK1/PARKIN signaling and mitochondrial quality control. BAG2 stabilizes PINK1 by decreasing its ubiquitination and allowing mitophagy induction [28,29]. BAG3, also known for its role in autophagy, maintains mitochondrial homeostasis by increasing PARKIN expression level [30]. Conversely, BAG5 impairs mitophagy by inhibiting PARKIN recruitment and favoring apoptosis [31]. BAG5 role in mitophagy is controversial because another study reported that the interaction between BAG5 and PINK1 decreases PINK1 ubiquitination and degradation [32]. These data indicate that the co-chaperones of the BAG family are involved in mitochondrial homeostasis, but the underlying mechanisms remain largely unknown. However, it appears that BAG2, BAG5 and BAG6 (this works) all stabilizes PINK1, suggesting a common mechanism.

To better understand how BAG6 affects mitophagy, the role of BAG6 intracellular localization needs to be better studied. Here, we showed that BAG6 is localized at the mitochondrial matrix in basal conditions, but relocates to the OMM after CCCP treatment. This relocation is compatible with the proposed BAG6 receptor function through its LIR2 domain. Similarly, the mitophagy receptor cardiolipin relocates from the IMM to the OMM after mitophagy induction [33]. However, on the basis of our results, we cannot exclude that BAG6 acts as an adaptor rather than a receptor and that its cytoplasmic form is recruited to the OMM after mitochondrial depolarization. However, its direct interaction with mitochondrial proteins seems improbable because BAG6 does not harbor a UBA or a UBD domain involved in the recognition of ubiquitylated mitochondrial proteins and essential for the adaptor function.

Another important question is how BAG6 is targeted to mitochondria. Indeed, the import of most mitochondrial proteins requires a pre-protein translocase at the outer mitochondrial membrane that cleaves the target protein after its translocation in the TOMM20

complex [34]. However, BAG6 has no mitochondrial targeting sequence. We cannot exclude that BAG6 might interact with a cytoplasmic co-factor responsible for its transport to the TOMM20 complex. Indeed, yeast two hybrid screening using TOMM20 as bait showed that BAG6 interacts with TOMM20 [35].

Our previous and current findings demonstrated the importance of BAG6 intracellular localization. In basal conditions, BAG6 maintains a pool of EP300 in the cytoplasm, leading to acetylation of ATG5, ATG7, ATG12 and LC3, thus inhibiting autophagy. After starvation, BAG6 induces the nuclear localization of EP300, decreasing ATG protein acetylation, but allowing TP53 acetylation and the expression of the pro-autophagic protein SESTRIN1 [17]. Here, we showed that mitochondrial BAG6 has a role in regulating mitochondrial structure and degradation. As mitophagy is inhibited during starvation [36] to limit mitochondrial degradation and prevent ATP deficiency, BAG6 role in the regulation of the links between autophagy and mitophagy should be investigated in the future.

To conclude, our work highlights new activities of BAG6 in regulating the mitochondrial structure and in mitophagy induction. As BAG6 is abnormally distributed during colon cancer ([37] and our unpublished data), it is important to determine the role of its intracellular localization and the consequences on both autophagy and mitophagy in physiological and pathological conditions.

Materials and Methods

Cells, plasmids, and reagents

MEFs were obtained and cultured as previously described [38].

LoVo cells, isolated from a left supraclavicular metastasis of colon cancer, were cultured in Roswell Park Memorial Institute medium supplemented with 10% FCS (NT), and SW480 cells were cultured in Dulbecco's modified Eagle's medium (DMEM) supplemented with 10% fetal calf serum (NT).

CQ (Sigma-Aldrich, St Louis, MO, USA) was used at 40 μ M for 6h or 24h depending on the experiment (see legends). CCCP (Abcam, Cambridge, UK) was used at 30 μ M for the indicated time (see figures) depending on the experiment. Indeed, the measurement of the degradation of mitochondrial markers by western blot required a 24h treatment. OA

LoVo cells were transfected with Lipofectamine 2000 according to the manufacturer's instructions (Invitrogen, Life Technologies, Carlsbad, CA, USA). Transfection efficiency was assayed by counting the number of cells transfected with a GFP encoding plasmid (GFP staining vs with light microscopy).

Plasmids

Plasmids encoding WT and mutant BAG6 variants were obtained as previously described (Sebti et al., 2014b). The PCI-BAG6 WT plasmid was used for site-directed mutagenesis of the LIR domains using the Phusion Site-Directed Mutagenesis Kit (ThermoFisher) and the following primers: BAG6 LIR1 Forward: 5' CCT TCC CCT GCG GAG GCT GTC GAG GCG CTC CAG GAG CTA CAG C 3' and BAG6 LIR1 Reverse: 5' GCT GTA GCT CCT GGA GCG CCT CGA CAG CCT CCG CAG GGG AAG G 3'; BAG6 LIR2 Forward: 5' GCA GCT GCA

GTC CCC CCA GAA GCG GTC CCT GCT ATC CAG CAG GAC ATT C 3', and BAG6 LIR2 Reverse: 5' GAA TGT CCT GCT GGA TAG CAG GGA CCG CTT CTG GGG GGA CTG CAG CTG C 3'.

Mitochondrial and cytoplasmic fraction isolation

The protocol for isolation of mitochondrial and cytoplasmic cell fractions was adapted from that described by Christian Frezza, et al. [39]. Briefly, cells were resuspended in mitochondrial isolation buffer (0.2M sucrose, 0.1mM TRIS/MOPS, 10 μ M EGTA/Tris) and disrupted with a dounce homogenizer, followed by centrifugation at 600 g at 4°C for 10min to discard nuclei and cell debris. The resulting pellets contained nuclei, whereas supernatants were centrifuged again at 7000 g at 4°C for 10min. Pellets contained the crude mitochondrial-enriched fractions, whereas supernatants contained the cytoplasmic/microsomal fractions. For experiments using cytoplasmic and crude mitochondrial fractions, equal amounts of proteins (quantified with the BCA Kit, Thermo Fisher Scientific) were analyzed by western blotting and probed with the indicated antibodies.

Proteinase K assay – Sub-mitochondrial localization

After mitochondrial isolation, mitochondria were incubated with 2.5 μ g/ml of PK for 10min after, or not, swelling in 10mM HEPES-KOH pH 7.4 that contained 1mM EDTA. PK digestion of mitochondrial proteins was stopped with 1mM PMSF. When indicated, 0.5% (v/v) Triton X-100 was added before PK treatment. Samples were precipitated by addition of trichloroacetic acid and analyzed by SDS-PAGE and immunoblotting using antibodies against mitochondrial markers as controls.

Fluorescence imaging

SW480 cells were fixed in Paraformaldehyde 1% for 10 min and then permeabilized in 0.1% Triton X-100 (room temperature, 30 min), then incubated in 5% BSA (37°C, 1h), and stained with an anti-mouse TOMM20 (Santa Cruz sc-17764, 1/100) and anti-BAG6 antibody (rabbit polyclonal, 26417-1-AP, Proteintech, 1/100). Nuclei were stained with 5µg/ml Hoechst dye (#33342 ThermoFisherScientific) at 37°C for 1h. Goat anti-rabbit Alexa Fluor 568 (red) (#A-11011, 1/1000; ThermoFisherScientific, Waltham, MA, USA) and goat anti-mouse Alexa Fluor 488 (green) (#A-11029, 1/1000; Thermo Fisher Scientific, Waltham, MA, USA) (diluted in 5% BSA) were added for 1h to detect BAG6 and TOMM20, respectively. Images were acquired with a Zeiss AxioCam MRm digital camera and analyzed with the Axiovision software.

Mitochondrial mass was measured by co-staining LoVo cells with the MitoTracker™ Red FM dye (20µM) and DAPI for 1h. When required, cells were incubated with 40 µM chloroquine for 6h. The intensity of the red fluorescence per cell was quantified with a Celigo Imaging cytometer (Nexcelom).

Immunoprecipitation

To immunoprecipitate WT or mutant (LIR1 and LIR2) BAG6, cells were lysed in lysis buffer [50mM Hepes pH 7.5, 150mM NaCl, 1.5mM MgCl₂, 100mM NaF, 10mM NaPPi, 1mM EDTA, 10% glycerol, 1% Triton X-100, and protease inhibitors) (Complete, Roche Applied Science, Indianapolis, IN, USA] at 4°C for 1h, and then overnight immunoprecipitation was performed at 4°C with a rabbit polyclonal anti-BAG6 antibody (1:2000; [38]). Protein A Sepharose beads (Amersham Biosciences, GE Healthcare, Waukesha, WI, USA) were added at 4°C for 2h and then washed three times with washing buffer (50mM Hepes pH 7.5, 150mM NaCl, 1mM

EDTA, 10% glycerol and 1% Triton X-100). Immunoprecipitated proteins were separated on SDS-PAGE, and BAG6 and LC3 were detected by immunoblotting.

Western blotting

Western blotting was performed with antibodies against PINK1 (1:1000; #BC100-494, Novus Biotechnologies), LC3 (1:5000, #L7543; Sigma-Aldrich Aldrich, St Louis, MO, USA), TFAM (#8076), DRP-1 (#8570), DRP-1 phosphorylated at S616 (#4494), PARKIN (#2132), GAPDH (14C10, #2118), histone H3 (D1H2, #4499) and phosphorylated-ubiquitinated proteins on S65 (#37642) (all 1:1000, Cell Signaling Technology, Danvers, MA, USA), TOMM20 (1:1000, #sc-17764; Santa Cruz Biotechnology, Inc, Santa Cruz, CA, USA), TIM23 (1:1000; #611223) and calnexin (#610523) from BD Biosciences, and tubulin (1:1000; #62204, Pierce, Thermo Fisher Scientific Inc., Rockford, IL, USA), For all figures, the anti-BAG6 antibody was Santa Cruz (1:2000; #sc-365928) except for Fig 2D and Fig 4A (SDIX, #3023.00.02 (1:1000)). Similarly, the anti-TOMM20 antibody was #sc-17764 from Santa Cruz Biotechnology (1:1000) for all figures, but for Fig. 4A (#sc-11415, 1:500).

Images were acquired with the GBOX imaging system (Syngene, Cambridge, USA) and the GeneSys software that allows the acquisition during the linear phase, avoiding saturation.

Transmission Electron Microscopy

Cells were immersed in a solution of 2.5% glutaraldehyde in Sorensen's buffer (0.1M, pH 7.4) overnight at 4 °C. After a rinse in Sorensen's buffer, cells were postfixed in a 0.5% osmic acid for 2 h in the dark at room temperature. After two rinses in Sorensen's buffer, the cells were dehydrated in a graded series of ethanol solutions (30–100%). The cells were embedded in EMbed 812 using a Leica EM AMW automated microwave tissue processor for electron

microscopy. Thin sections (70 nm, obtained with a Leica-Reichert Ultracut E microtome) were collected at different levels of each block. These sections were counterstained with uranyl acetate and observed with a Hitachi 7100 transmission electron microscope at the Centre de Ressources en Imagerie Cellulaire de Montpellier, Montpellier, France.

Statistical analysis

Data were analyzed using the Student's *t*-test. P values <0.001, 0.01, and 0.05 versus controls were considered significant and were noted as ***, **, and *, respectively. All results were reported as the mean \pm standard deviation (SD), with error bars to show the SD.

Legends

Figure 1: BAG6 is localized in mitochondria in SW480 and BAG6-transfected LoVo cells.

(A) Cell fractions from SW480 colon cancer cells were immunoblotted with anti-BAG6, anti-tubulin (cytoplasmic marker) and anti-TFAM (mitochondrial marker) antibodies. Mito, mitochondrial fraction.

(B) SW480 cells were incubated with anti-TOMM20 (green) and anti-BAG6 (red) antibodies. Nuclei were stained with Hoechst. Images were acquired with a Zeiss AxioCam MRm digital camera and the Axiovision software. Size bar represents 10 μm .

(C) Mitochondria from SW480 cells cultured in complete medium were isolated and fractionated in the presence or absence of 0.25 μM PK, after or not swelling and incubation with 0.1% Triton X-100 for 30 min (as indicated). Immunoblotting was performed with anti-BAG6, anti-TOMM20 (OMM protein), anti-TIM23 (IMM protein), and anti-TFAM (mitochondrial matrix protein) antibodies.

(D) The indicated cell fractions from LoVo cells transfected with EV or BAG6 plasmids were immunoblotted with anti-BAG6, anti-calnexin (ER marker), and anti-tubulin (cytoplasm marker) antibodies.

(E) BAG6 transfected LoVo cells were incubated with anti-TOMM20 (green) and anti-BAG6 (red) antibodies. Nuclei were stained with Hoechst. Z-stacks images were acquired with a Zeiss AxioImager Z2 microscope equipped with a Photometrics CoolSnap HQ2 camera. Acquired Z-stacks were then deconvolved with AutoQuant X3 (Media Cybernetics). Arrows represents examples of co-localisation spots. Size bar represents 10 μm .

(F) BAG6-transfected LoVo cells were incubated or not with 20 μ M CCCP for 6h. Mitochondria were isolated and fractionated in the presence or absence of 0.25 μ M PK, after or not swelling and incubation with 0.1% Triton X-100 for 30min, as indicated. Immunoblotting was performed by using anti-BAG6, anti-TOMM20 (OMM protein), anti-TIM23 (IMM protein), and anti-TFAM (mitochondrial matrix protein) antibodies.

Figure 2: The overexpression of BAG6 in BAG6-LoVo null cells decreases the number of mitochondria in a chloroquine-dependent manner

(A) Representative ultrastructural images of EV- or and BAG6-transfected LoVo cells after incubation or not (NT) with 20 μ M CCCP for 8h.

(B) Quantification of the size of 200 mitochondria using the ImageJ software (μ M). ***P \leq 0.001 vs. BAG6 versus EV transfected cells.

(C) The number of mitochondria per cell was quantified in 200 cells transfected with EV or PCI-BAG6 and incubated or not (NT) with 20 μ M CCCP for 8h.

(C) Quantification of the fluorescence signal (MitoTracker™ Red FM) in LoVo cells transfected with EV or BAG6 and incubated or not (NT) with 20 μ M CCCP for 6h and with or without 40 μ M CQ for 6h (Celigo Cytometer imager, Nexcelom).

(D) LoVo cells transfected with EV or BAG6 were incubated or not (NT) with 30 μ M CCCP and/or μ M CQ for 24h. Total protein extracts were immunoblotted with anti-BAG6, anti-TFAM, - and anti-GAPDH antibodies.

(E) Quantification of (D) using the ImageJ software.

Figure 3: Endogenous BAG6 is essential for mitophagy in SW480 cells

(A) SW480-shLuc and SW480-shBAG6 cells were treated or not (NT) with 30 μ M CCCP for 24h and then were incubated with anti-TOMM20 (green) and the nuclei stained with Hoechst. Z-stacks images were acquired with a Zeiss AxioImager Z2 microscope equipped with a Photometrics CoolSnap HQ2 camera. Acquired Z-stacks were then deconvolved with AutoQuant X3 (Media Cybernetics). Size bar represents 5 μ m.

(B) Box plot of at least 50 cells from (A) were analyzed per condition. Similar results were observed in three independent experiments. **** $p < 0.0001$; Mann-Whitney U test. Show here is median and interquartile. X marks the mean.

(C) SW480-shLuc and SW480-shBAG6 cells were treated or not with 30 μ M CCCP for 24h were incubated or not (NT) with 30 μ M CCCP and/or μ M CQ for 24h. Total protein extracts were immunoblotted with anti-BAG6, anti-TFAM, - and anti-GAPDH antibodies.

(E) Quantification of (D) using the ImageJ software.

BAG6 promotes mitochondrial fission.

(B) 30 μ g of indicated cell fractions of LoVo cells transfected with EV or a BAG6 construct were immunoblotted with antibodies against DRP1, DRP1 phosphorylated (P) at S616, TFAM (mitochondrial marker), and tubulin (cytoplasmic marker).

(C) Quantification of (B) by using Image J software.

Fig.4: BAG6 induces the PINK1/PARKIN signaling pathway

(A) 30 μ g of indicated cell fractions of LoVo cells transfected with EV or BAG6 and incubated or not (NT) with 30 μ M CCCP for 8h were immunoblotted with anti-BAG6, anti-PINK1, anti-PARKIN, anti-TOMM20, anti-tubulin and anti-histone H3 antibodies.

(B) Quantification of the signal intensity of mitochondrial PINK1 in (A) using the Image J software.

(C) Quantification of the signal intensity of mitochondrial PARKIN in (A) using the Image J software.

(D) Cell lysates (L) and mitochondria (M) extracted from LoVo cells transfected with EV or a BAG6 plasmid and incubated or not (NT) with 30 μ M CCCP for 8h were immunoblotted with an anti-phospho-ubiquitin antibody. LC, loading control (Ponceau staining of the blot).

(E) Quantification of the signal intensity in (D) using the Image J software.

Fig.5: The LIR2 domain of BAG6 is responsible for its interaction with LC3 and for mitophagy induction

(A) Schematic representation of BAG6 sequence with the UBL domain and the two LIR domains with the mutations introduced by site-directed mutagenesis.

(B) The indicated cell fractions from LoVo cells transfected with EV or BAG6 plasmids were immunoblotted with anti-BAG6, anti-calnexin (ER marker), and anti-tubulin (cytoplasm marker) antibodies. (A) Cell fractions from LoVo cells transfected with a plasmid encoding for BAG6 or BAG6-LIR1 or BAG6 LIR2 immunoblotted with anti-BAG6, anti-tubulin (cytoplasmic marker), anti-TFAM (mitochondrial marker) and anti-histone H3 antibodies. Mito, mitochondrial fraction.

(C) Representative ultrastructural images of EV-, BAG6 WT-, BAG6 LIR1- and BAG6 LIR2-transfected LoVo cells incubated or not (NT) with 20 μ M CCCP.

(D) The number of mitochondria per cell was quantified in 200 cells from the different conditions.

(E) Protein extracts from LoVo cells transfected with EV, WT BAG6, or mutant BAG6 (BAG6 LIR1 Y276A/V279A, or BAG6 LIR2W1018A/1021A) treated with 30 μ M for 24 h were immunoblotted with anti-BAG6, anti-TFAM and anti-GAPDH antibodies.

(F) Quantification of (E) using the ImageJ software.

(G) Protein extracts from LoVo cells transfected with EV, WT BAG6, or mutant BAG6 (BAG6 LIR1 Y276A/V279A, or BAG6 LIR2W1018A/1021A) were immunoprecipitated with an anti-BAG6 antibody. Immunoprecipitated proteins were revealed with anti-LC3 and anti-BAG6 antibodies.

Legend Supplemental Figures

Figure S1: BAG6 is localized in mitochondria.

(A) The indicated cell fractions from HEK293T cells were immunoblotted with anti-BAG6, anti-tubulin (cytoplasmic marker), anti-TOMM20 (mitochondrial marker), and anti-histone H3 (nuclear marker) antibodies. **(B)** The indicated cell fractions from MEFs were immunoblotted with anti-BAG6, anti-tubulin (cytoplasmic marker), anti-TFAM (mitochondrial marker), and anti-histone H3 (nuclear marker) antibodies.

BAG6 promotes mitochondrial fission.

(B) 30 μ g of indicated cell fractions of LoVo cells transfected with EV or a BAG6 construct were immunoblotted with antibodies against DRP1, DRP1 phosphorylated (P) at S616, TFAM (mitochondrial marker), and tubulin (cytoplasmic marker).

(C) Quantification of (B) by using Image J software.

Acknowledgements

We thank the Centre de Ressources en Imagerie Cellulaire and C. Cazevieille, for her technical assistance with ultrastructural data. We thank Patrice Codogno (INEM, Paris, France) for helpful discussions. We are also grateful to Claude Sardet for his support during the redaction of the manuscript.

This work is dedicated to the memory of Beth Levine.

Disclosure statement

No potential conflict of interest was reported by the authors.

Funding

This work is supported by the Institut National de la Santé et de la Recherche Médicale, by the ARC fondation (S.P.), La Ligue Régionale contre Le Cancer (Comité de l'Hérault; S.P.). Dr Leila. El Kebriti is a recipient of a Nimes University Hospital graduate program fellowship

References

1. Gomes LC, Scorrano L (2013) Mitochondrial morphology in mitophagy and macroautophagy. *Biochim Biophys Acta* **1833**: 205–212.
2. Morita M, Prudent J, Basu K, Goyon V, Katsumura S, Hulea L, Pearl D, Siddiqui N, Strack S, McGuirk S, et al. (2017) mTOR Controls Mitochondrial Dynamics and Cell Survival via MTFP1. *Mol Cell* **67**: 922–935.e5.
3. Rambold AS, Lippincott-Schwartz J (2011) Mechanisms of mitochondria and autophagy crosstalk. *Cell Cycle* **10**: 4032–4038.
4. Kalvari I, Tsompanis S, Mulakkal NC, Osgood R, Johansen T, Nezis IP, Promponas VJ (2014) iLIR: A web resource for prediction of Atg8-family interacting proteins. *Autophagy* **10**: 913–925.
5. Novak I, Kirkin V, McEwan DG, Zhang J, Wild P, Rozenknop A, Rogov V, Löhr F, Popovic D, Occhipinti A, et al. (2010) Nix is a selective autophagy receptor for mitochondrial clearance. *EMBO Rep* **11**: 45–51.
6. Hanna RA, Quinsay MN, Orogo AM, Giang K, Rikka S, Gustafsson ÅB (2012) Microtubule-associated Protein 1 Light Chain 3 (LC3) Interacts with Bnip3 Protein to Selectively Remove Endoplasmic Reticulum and Mitochondria via Autophagy. *J Biol Chem* **287**: 19094–19104.
7. Murakawa T, Yamaguchi O, Hashimoto A, Hikoso S, Takeda T, Oka T, Yasui H, Ueda H, Akazawa Y, Nakayama H, et al. (2015) Bcl-2-like protein 13 is a mammalian Atg32 homologue that mediates mitophagy and mitochondrial fragmentation. *Nat Commun* **6**: 7527.
8. Wei Y, Chiang W-C, Sumpter R, Mishra P, Levine B (2017) Prohibitin 2 Is an Inner Mitochondrial Membrane Mitophagy Receptor. *Cell* **168**: 224–238.e10.
9. Bhujabal Z, Birgisdottir ÅB, Sjøttem E, Brenne HB, Øvervatn A, Habisov S, Kirkin V, Lamark T, Johansen T (2017) FKBP8 recruits LC3A to mediate Parkin-independent mitophagy. *EMBO reports* **18**: 947–961.
10. Okamoto K, Kondo-Okamoto N, Ohsumi Y (2009) Mitochondria-anchored receptor Atg32 mediates degradation of mitochondria via selective autophagy. *Dev Cell* **17**: 87–97.
11. Montava-Garriga L, Ganley IG (2019) Outstanding Questions in Mitophagy: What We Do and Do Not Know. *J Mol Biol.*
12. Kazlauskaitė A, Kondapalli C, Gourlay R, Campbell DG, Ritorto MS, Hofmann K, Alessi DR, Knebel A, Trost M, Muqit MMK (2014) Parkin is activated by PINK1-dependent phosphorylation of ubiquitin at Ser65. *Biochem J* **460**: 127–139.
13. Koyano F, Okatsu K, Kosako H, Tamura Y, Go E, Kimura M, Kimura Y, Tsuchiya H, Yoshihara H, Hirokawa T, et al. (2014) Ubiquitin is phosphorylated by PINK1 to activate parkin. *Nature* **510**: 162–166.
14. Kawahara H, Minami R, Yokota N (2013) BAG6/BAT3: emerging roles in quality control for nascent polypeptides. *J Biochem* **153**: 147–160.
15. Lee J-G, Ye Y (2013) Bag6/Bat3/Scythe: a novel chaperone activity with diverse regulatory functions in protein biogenesis and degradation. *Bioessays* **35**: 377–385.
16. Sebti S, Prébois C, Pérez-Gracia E, Bauvy C, Desmots F, Gongora C, Pirot N, Bach A-S, Hubberstey A, Palissot V, et al. (2014) BAG6/BAT3 modulates autophagy by affecting EP300/p300 intracellular localization. *Autophagy* **10**: 0–1.
17. Sebti S, Prébois C, Pérez-Gracia E, Bauvy C, Desmots F, Pirot N, Gongora C, Bach A-S, Hubberstey AV, Palissot V, et al. (2014) BAT3 modulates p300-dependent acetylation of p53 and autophagy-related protein 7 (ATG7) during autophagy. *Proc Natl Acad Sci USA* **111**: 4115–4120.
18. Saita S, Ishihara T, Maeda M, Iemura S-I, Natsume T, Mihara K, Ishihara N (2016) Distinct types of protease systems are involved in homeostasis regulation of mitochondrial morphology via balanced fusion and fission. *Genes Cells* **21**: 408–424.
19. Hayashishita M, Kawahara H, Yokota N (2019) BAG6 deficiency induces mis-distribution of mitochondrial clusters under depolarization. *FEBS Open Bio* **9**: 1281–1291.

20. Wai T, Saita S, Nolte H, Müller S, König T, Richter-Dennerlein R, Sprenger H-G, Madrenas J, Mühlmeister M, Brandt U, et al. (2016) The membrane scaffold SLP2 anchors a proteolytic hub in mitochondria containing PARL and the i-AAA protease YME1L. *EMBO Rep* **17**: 1844–1856.
21. Claessen JHL, Ploegh HL (2011) BAT3 guides misfolded glycoproteins out of the endoplasmic reticulum. *PLoS ONE* **6**: e28542.
22. Mauthe M, Orhon I, Rocchi C, Zhou X, Luhr M, Hijlkema K-J, Coppes RP, Engedal N, Mari M, Reggiori F (2018) Chloroquine inhibits autophagic flux by decreasing autophagosome-lysosome fusion. *Autophagy* **14**: 1435–1455.
23. Klionsky DJ, Abdelmohsen K, Abe A, Abedin MJ, Abeliovich H, Acevedo Arozena A, Adachi H, Adams CM, Adams PD, Adeli K, et al. (2016) Guidelines for the use and interpretation of assays for monitoring autophagy (3rd edition). *Autophagy* **12**: 1–222.
24. Yoshii SR, Kishi C, Ishihara N, Mizushima N (2011) Parkin mediates proteasome-dependent protein degradation and rupture of the outer mitochondrial membrane. *J Biol Chem* **286**: 19630–19640.
25. Liu L, Feng D, Chen G, Chen M, Zheng Q, Song P, Ma Q, Zhu C, Wang R, Qi W, et al. (2012) Mitochondrial outer-membrane protein FUNDC1 mediates hypoxia-induced mitophagy in mammalian cells. *Nat Cell Biol* **14**: 177–185.
26. Zhu Y, Massen S, Terenzio M, Lang V, Chen-Lindner S, Eils R, Novak I, Dikic I, Hamacher-Brady A, Brady NR (2013) Modulation of serines 17 and 24 in the LC3-interacting region of Bnip3 determines pro-survival mitophagy versus apoptosis. *J Biol Chem* **288**: 1099–1113.
27. Twig G, Elorza A, Molina AJA, Mohamed H, Wikstrom JD, Walzer G, Stiles L, Haigh SE, Katz S, Las G, et al. (2008) Fission and selective fusion govern mitochondrial segregation and elimination by autophagy. *EMBO J* **27**: 433–446.
28. Che X, Tang B, Wang X, Chen D, Yan X, Jiang H, Shen L, Xu Q, Wang G, Guo J (2013) The BAG2 protein stabilises PINK1 by decreasing its ubiquitination. *Biochem Biophys Res Commun* **441**: 488–492.
29. Qu D, Hage A, Don-Carolis K, Huang E, Joselin A, Safarpour F, Marcogliese PC, Rousseaux MWC, Hewitt SJ, Huang T, et al. (2015) BAG2 Gene-mediated Regulation of PINK1 Protein Is Critical for Mitochondrial Translocation of PARKIN and Neuronal Survival. *J Biol Chem* **290**: 30441–30452.
30. Tahrir FG, Knezevic T, Gupta MK, Gordon J, Cheung JY, Feldman AM, Khalili K (2017) Evidence for the Role of BAG3 in Mitochondrial Quality Control in Cardiomyocytes. *J Cell Physiol* **232**: 797–805.
31. De Snoo ML, Friesen EL, Zhang YT, Earnshaw R, Dorval G, Kapadia M, O’Hara DM, Agapova V, Chau H, Pellerito O, et al. (2019) Bcl-2-associated athanogene 5 (BAG5) regulates Parkin-dependent mitophagy and cell death. *Cell Death Dis* **10**: 907.
32. Wang X, Guo J, Fei E, Mu Y, He S, Che X, Tan J, Xia K, Zhang Z, Wang G, et al. (2014) BAG5 protects against mitochondrial oxidative damage through regulating PINK1 degradation. *PLoS ONE* **9**: e86276.
33. Chu CT, Ji J, Dagda RK, Jiang JF, Tyurina YY, Kapralov AA, Tyurin VA, Yanamala N, Shrivastava IH, Mohammadyani D, et al. (2013) Cardiolipin externalization to the outer mitochondrial membrane acts as an elimination signal for mitophagy in neuronal cells. *Nat Cell Biol* **15**: 1197–1205.
34. Harbauer AB, Zahedi RP, Sickmann A, Pfanner N, Meisinger C (2014) The protein import machinery of mitochondria—a regulatory hub in metabolism, stress, and disease. *Cell Metab* **19**: 357–372.
35. Stelzl U, Worm U, Lalowski M, Haenig C, Brembeck FH, Goehler H, Stroedicke M, Zenkner M, Schoenherr A, Koeppen S, et al. (2005) A human protein-protein interaction network: a resource for annotating the proteome. *Cell* **122**: 957–968.
36. Gomes LC, Di Benedetto G, Scorrano L (2011) During autophagy mitochondria elongate, are spared from degradation and sustain cell viability. *Nat Cell Biol* **13**: 589–598.
37. Wu W, Song W, Li S, Ouyang S, Fok KL, Diao R, Miao S, Chan HC, Wang L (2012) Regulation of apoptosis by Bat3-enhanced YWK-II/APLP2 protein stability. *J Cell Sci* **125**: 4219–4229.

38. Desmots F, Russell HR, Lee Y, Boyd K, McKinnon PJ (2005) The reaper-binding protein scythe modulates apoptosis and proliferation during mammalian development. *Mol Cell Biol* **25**: 10329–10337.
39. Frezza C, Cipolat S, Scorrano L (2007) Organelle isolation: functional mitochondria from mouse liver, muscle and cultured fibroblasts. *Nat Protoc* **2**: 287–295.

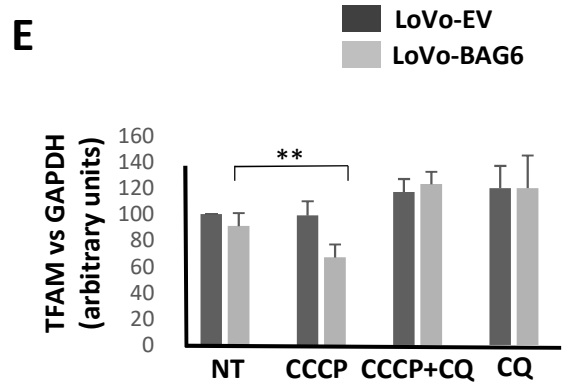
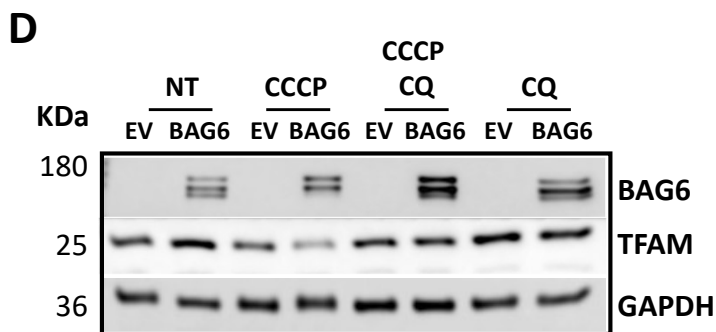
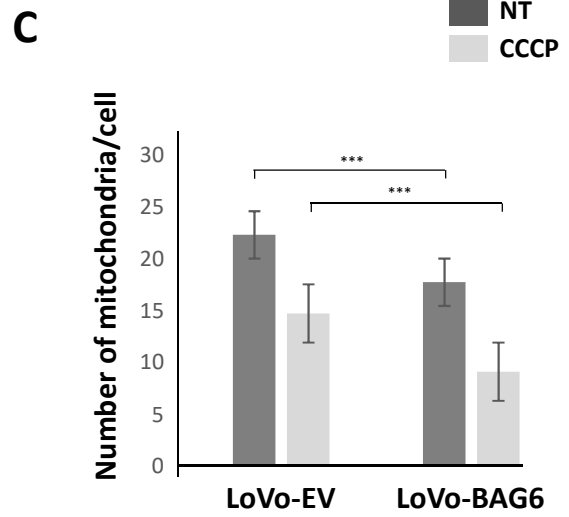
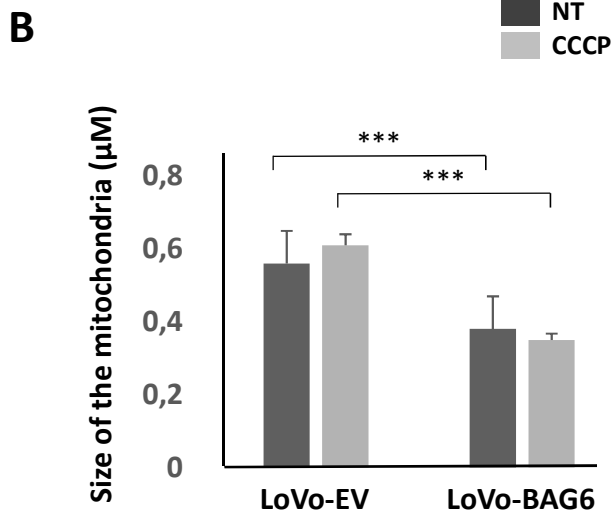
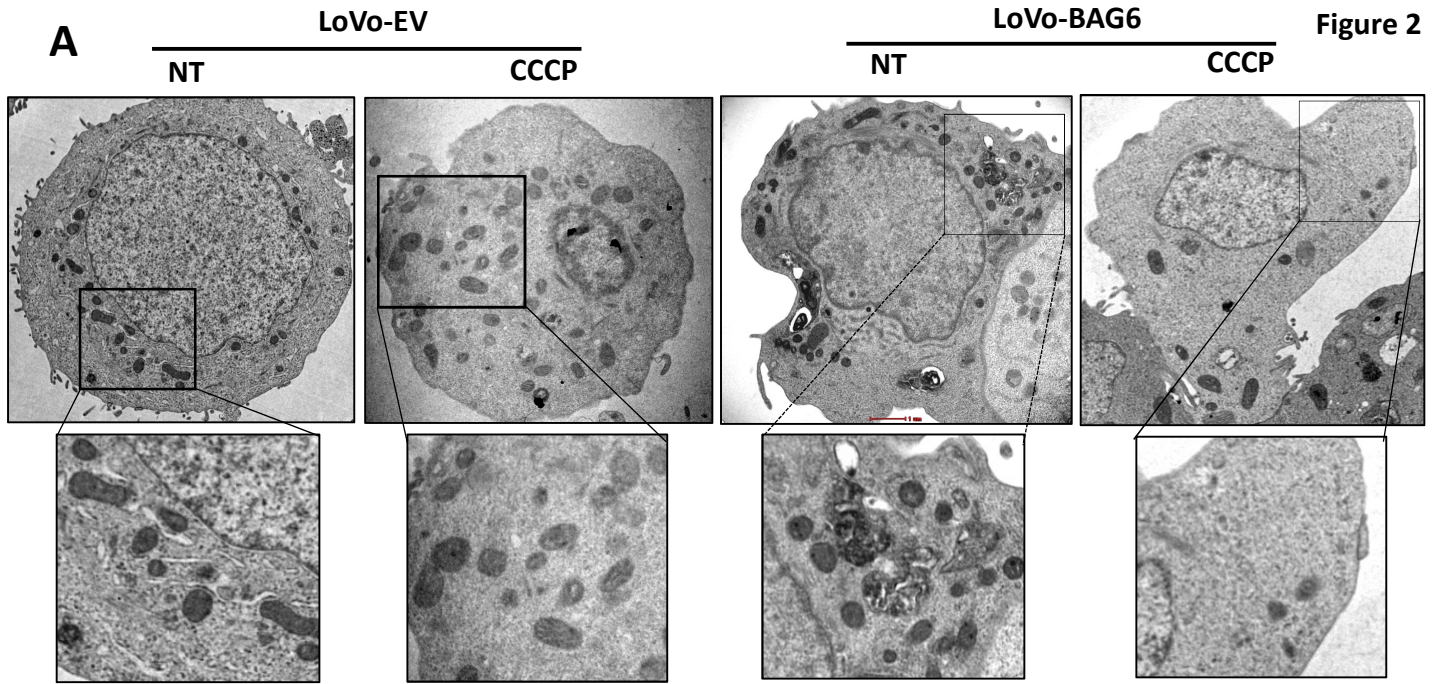


Figure 3

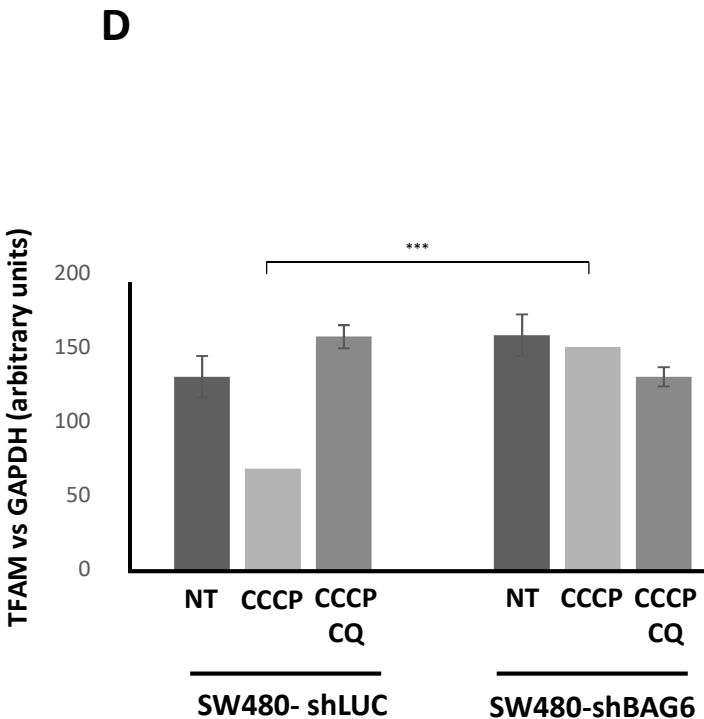
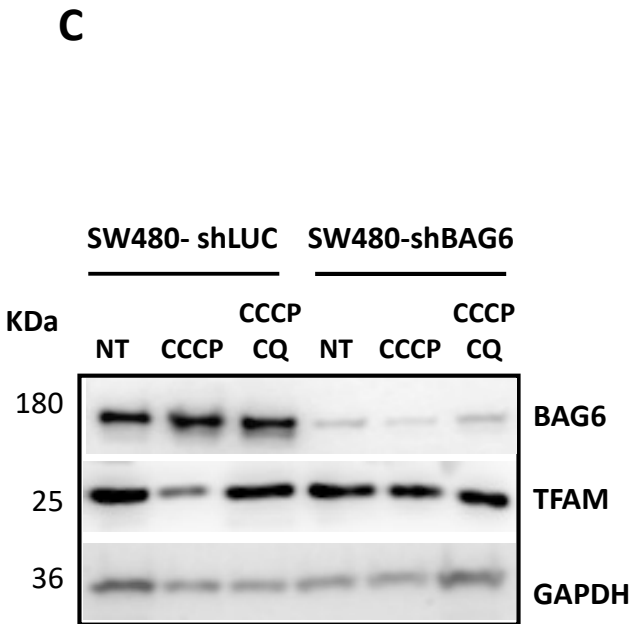
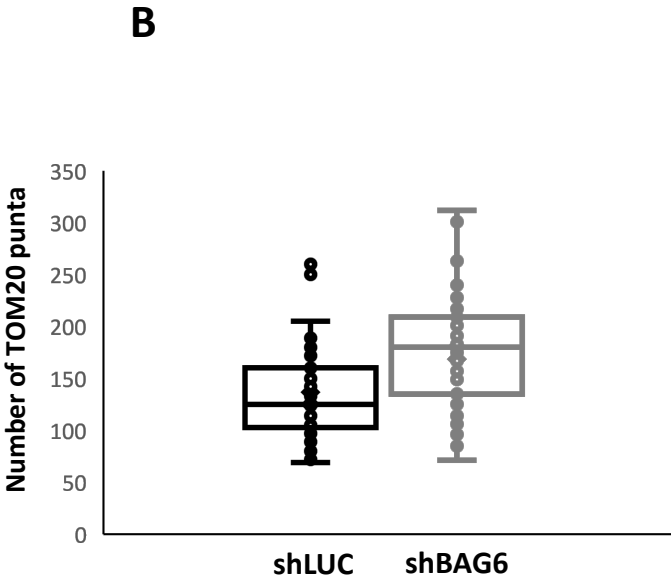
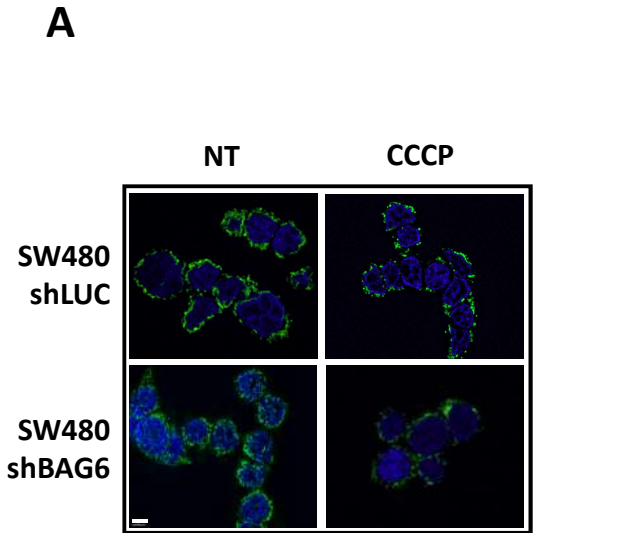


Figure 4

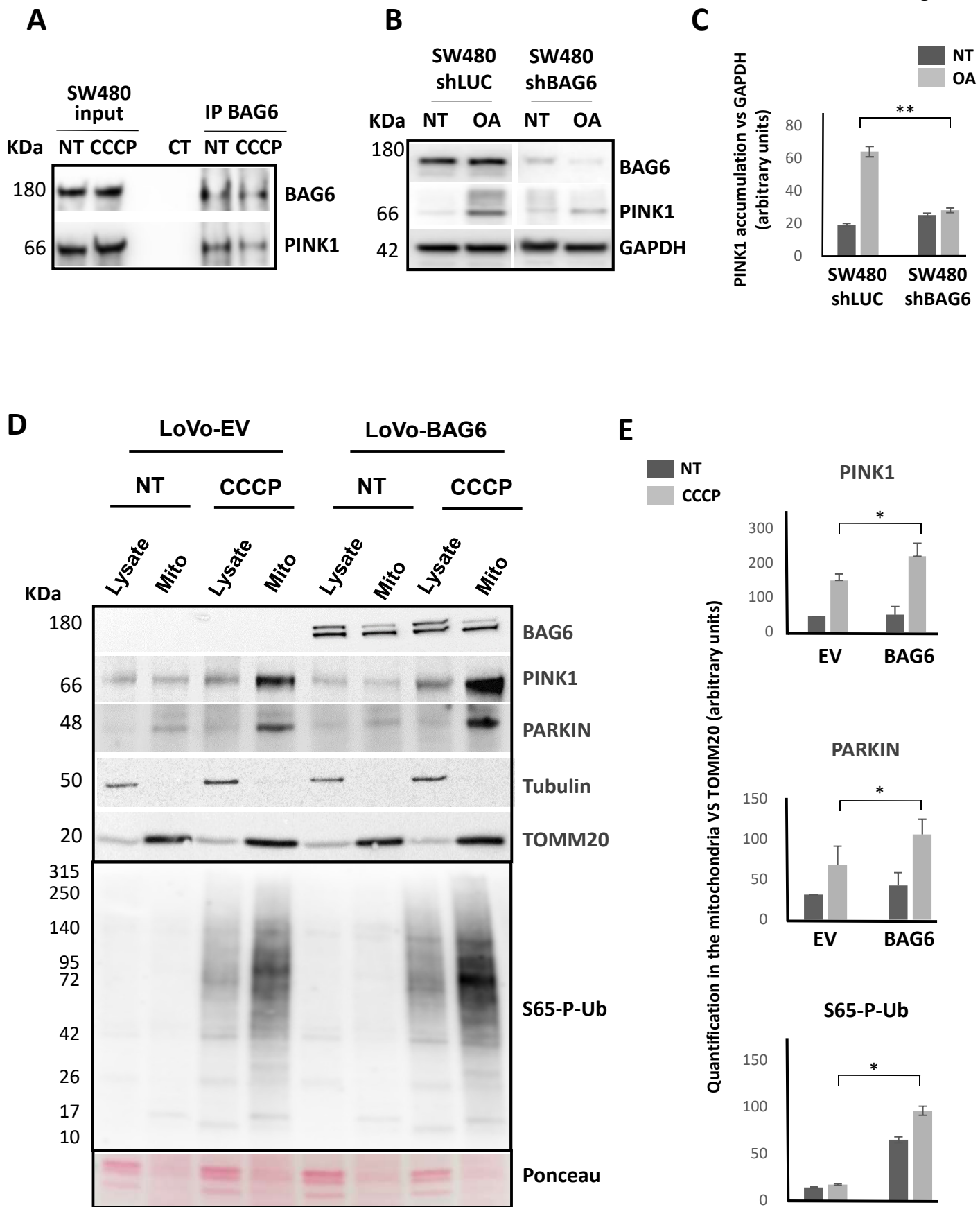


Figure 5

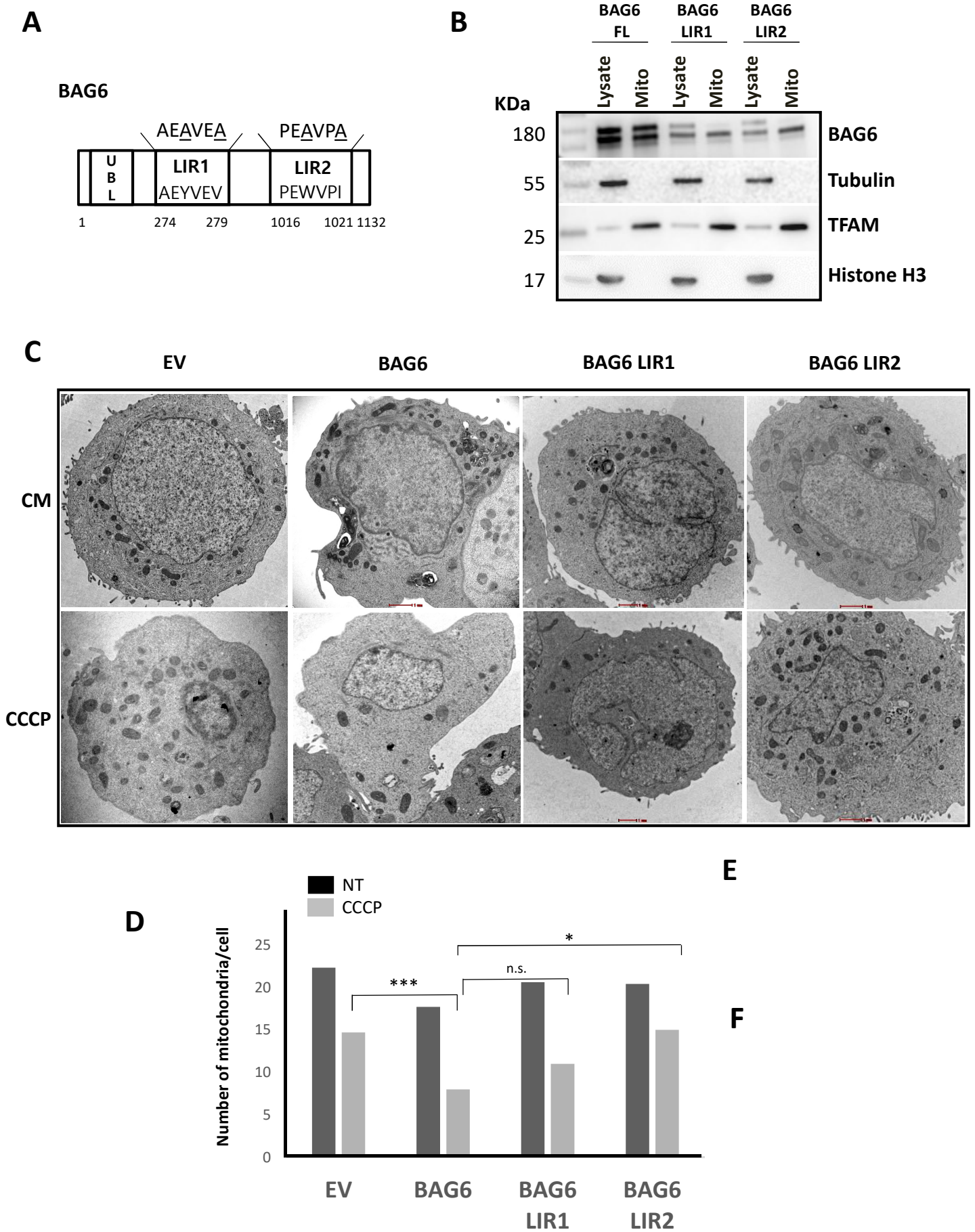
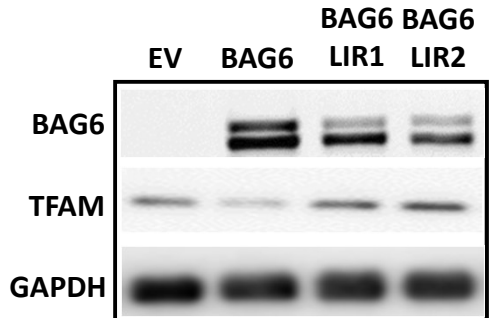
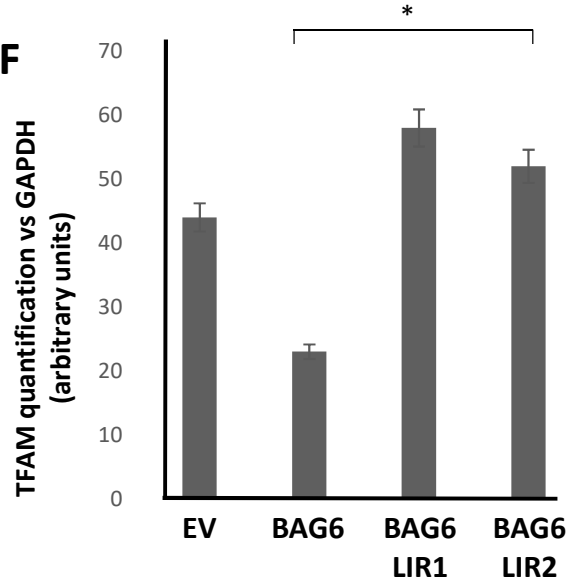


Figure 5

E



F



G

